(66)

Bechtel Nevada

DOE/NV/11718-021
UC-702
JUNE 1997

THE
REMOTE
SENSING
LABORATORY
OPERATED BY BECHTEL NEVADA
FOR THE U.S. DEPARTMENT OF ENERGY

25

AN AERIAL RADIOLOGICAL SURVEY OF THE NINE MILE POINT AND JAMES FITZPATRICK NUCLEAR POWER PLANTS AND SURROUNDING AREAS

LYCOMING, NEW YORK

DATE OF SURVEY: OCTOBER 12–17, 1995

DISCLAIMER

Bechtel Nevada

DOE/NV/11718-021
JUNE 1997

AN AERIAL RADIOLOGICAL SURVEY OF THE NINE MILE POINT AND JAMES FITZPATRICK NUCLEAR POWER PLANTS AND SURROUNDING AREAS

LYCOMING, NEW YORK

DATE OF SURVEY: OCTOBER 12–17, 1995

A. E. Proctor
Project Scientist

REVIEWED BY

Harvey W. Clark Jr.
H. W. Clark, Jr., Manager
Radiation Sciences

This Document is UNCLASSIFIED

Thomas M. Hayes
T. M. Hayes
Authorized Derivative Classifier

This work was performed for the U.S. Nuclear Regulatory Commission by EG&G Energy Measurements, Inc., and Bechtel Nevada through an Economy Act Order transfer of funds to Contract Number DE-AC08-93NV11265 (EG&G/EM) and Contract Number DE-AC08-96NV11718 (Bechtel Nevada) with the U.S. Department of Energy.

ABSTRACT

Terrestrial radioactivity surrounding the Nine Mile Point and James FitzPatrick Nuclear Power Plants was measured using aerial radiological surveying techniques. The purpose of this survey was to document exposure rates near the plants and to identify unexpected, man-made radiation sources within the survey area. The surveyed area included land areas within a three-mile radius of the plant sites. Data were acquired using an airborne detection system that employed sodium iodide, thallium-activated detectors. Exposure-rate and photopeak counts were computed from these data and plotted on aerial photographs of the survey area. Several ground-based exposure measurements were made for comparison with the aerial survey results. Exposure rates in areas surrounding the plant sites varied from below 5.5 to 9 microroentgens per hour. Man-made radiation was found to be higher than background levels at the plant sites. Radiation due to nitrogen-16, which is produced in the steam cycle of boiling-water reactors, was the primary source of activity found at the plant sites. Areas away from the plant sites were free of detectable man-made radioactivity.

CONTENTS

Tables

Appendices

1.0 INTRODUCTION

An aerial radiological survey of both the Nine Mile Point and James FitzPatrick Nuclear Power Plant sites and surrounding areas was conducted during October 1995 by the Remote Sensing Laboratory (RSL) for the U.S. Nuclear Regulatory Commission. This survey is part of an ongoing effort to characterize radiation levels surrounding commercial nuclear power plants. Commercial plant sites are surveyed prior to initial criticality and periodically thereafter until the plant is decommissioned and the site is returned to nonnuclear uses.

The Nine Mile Point Plant and James FitzPatrick Plant use boiling-water reactors. Table 1 shows the operators of these reactors and their respective power outputs.

Previous aerial radiological surveys were performed in September 1969[1] and September 1972.[2] The 1969 survey was conducted before the reactors were operating. During the 1972 survey, only the Nine Mile Point Unit 1 reactor was operational. All three reactors were operational during the 1995 survey. There were no known outages or other activities that might have influenced the radiation measurements taken during the six-day survey.

The survey consisted of aerial measurements of both natural and man-made gamma radiation emanating from the terrestrial surface. The purpose of this survey was to measure the exposure rates near the plant and to determine if measurable contamination from the plants had spread outside plant site boundaries. Results are reported as radiation isopleths superimposed on aerial photographs and topographic maps of the area.

The RSL performs various types of radiological surveys for the U.S. Department of Energy (DOE) and other customers. The RSL's capabilities include an airborne radiological surveillance system called the Aerial Measuring System (AMS). Since its inception in 1958, the AMS program has carried out radiological surveys of nuclear power plants, processing plants for nuclear materials, and research laboratories. The AMS aircraft have been deployed to nuclear accident sites and in searches for lost radioactive sources. The AMS aircraft also fly mapping cameras and multispectral camera arrays for aerial photography and thermal mappers for infrared imagery. Survey operations are conducted at the request of various federal and state agencies.

2.0 SURVEY SITE DESCRIPTION

The Nine Mile Point and James FitzPatrick Nuclear Power Plant sites are located along the Lake Ontario shore, ten miles northeast of Oswego, New York. The two plant sites adjoin with the James FitzPatrick site located east of the Nine Mile Point site. Other nearby towns are Lycoming, Scriba, and Fulton. Syracuse is 35 miles south of the plant sites. Coordinates for the plant sites are latitude 43°31′18″ N and longitude 76°23′53″ W. Figure 1 shows the plant sites. The James FitzPatrick facility is in the foreground, and the two units and large cooling tower of the Nine Mile Point facility are shown in the background of this photograph. Appendix A provides a summary of the survey parameters.

Table 1. Nuclear Power Reactors within the Survey Area[a]

Reactor Designation	Initial Commercial Operation	Power Generation (MW[E])	Reactor Operator
Nine Mile Point Unit 1	12/69	610	Niagara Mohawk Power Corporation
Nine Mile Point Unit 2	04/88	1,143	Niagara Mohawk Power Corporation
James FitzPatrick	07/75	780	New York Power Authority

[a] "World List of Nuclear Power Plants," *Nuclear News*, March 1995.

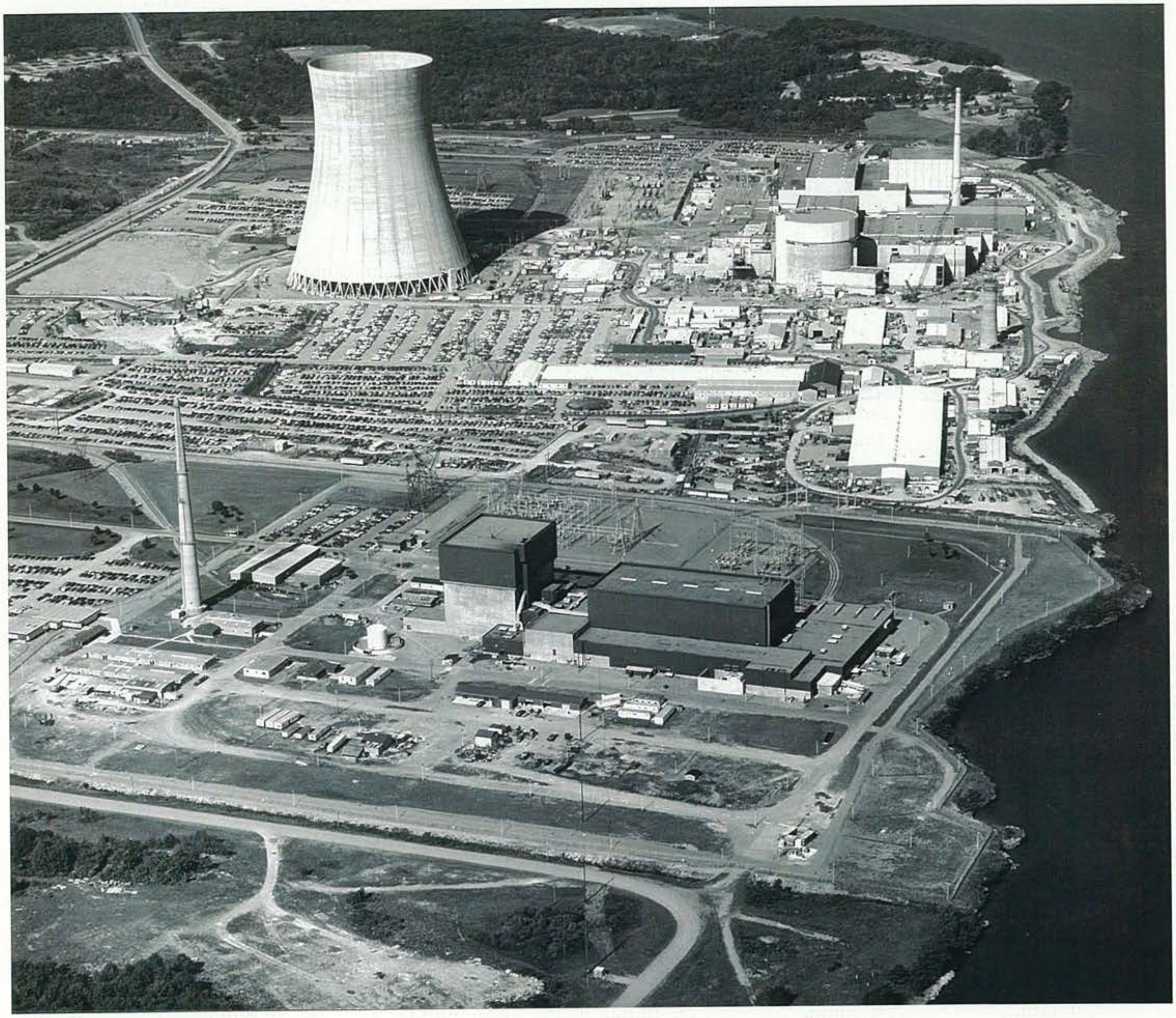

FIGURE 1. ***NINE MILE POINT/JAMES FITZPATRICK NUCLEAR POWER PLANT SURVEY SITE***

2.1 Topography and Land Use

The topography consists of rolling terrain with moist soil. Types of vegetation range from pasture to cultivated fields to forested areas. The majority of the trees are deciduous including some fruit trees in commercial orchards. Some swampy areas and areas covered with rotting vegetation were observed, but these comprised a small fraction of the survey area. The survey was completed in early fall while most of the leaves remained on the trees. There were no exposed rocks except for man-made rail beds and roads in several developed areas.

Except for several towns, the area is sparsely populated. Land uses include agriculture, forestry, small industry, and urban development. Urban development is found in Oswego, Fulton, and Scriba and in small developments scattered throughout the survey area.

2.2 Survey Area

The plant sites are located on the shoreline of Lake Ontario. The survey area extends south from the shoreline in an approximate semicircle with a three-mile radius centered on the plant. An area extending 1,000–1,500 ft (300–460 m) over Lake Ontario was surveyed to facilitate later data reduction.

3.0 SURVEY METHODS

Standard aerial radiation survey techniques developed for large-area gamma radiation surveys were used.[3] The survey methodology has been successfully applied to more than 300 individual surveys at various locations beginning in the late 1960s.

3.1 Aerial Radiation Measurements

A Messerschmitt-Bolkow-Blohm (MBB) BO-105 helicopter with externally mounted detector pods, shown in Figure 2, was used to collect the data. Figure 3 illustrates important details of the aerial radiological surveying process. Gamma-ray spectral data were acquired at uniform spacing along a series of parallel lines that were flown in a north–south direction at an altitude of 150 ft (46 m) above ground level (AGL) and at a line spacing of 250 ft (76 m). Data were acquired continuously along these lines and recorded in one-second intervals at an airspeed of 70 knots (36 m/s). This one-second interval corresponds to a 118-ft (36-m) data interval. During each interval, two gamma-ray spectra were accumulated from eight sodium iodide, thallium-activated, NaI(Tl), detectors. Other information such as air temperature, pressure, and altitude were also recorded during each interval.

FIGURE 2. *MBB BO-105 HELICOPTER WITH DETECTOR PODS*

The helicopter position was established by a Global Positioning System (GPS) operated in differential mode. Real-time aircraft positions were determined by an on-board GPS receiver, based on the measured position from GPS satellite data and a correction transmitted from a second GPS station located at a known position on the ground. The airborne GPS receiver provided continuous positional data to a microprocessor that reformatted the data for use in RSL's airborne, computerized data-logging systems. This on-board computer recorded the positional data and operated a steering indicator to aid the pilot in flying a set of equally spaced straight lines.

Real-time altitude measurements were made through a radar altimeter that measured the return time for a pulsed signal and converted this delay to aircraft altitude. For altitudes up to 2,000 ft (610 m), the manufacturer's stated accuracy is ± 2 ft (0.6 m) or ± 2 percent, whichever is greater. Altitude data were also recorded by the data-acquisition system so that variations in gamma signal strength caused by altitude fluctuations could be identified.

3.2 Data-Acquisition System

The detection system consists of two rectangular aluminum pods. Each pod contains four 2- $\times$ 4- $\times$ 16-in down-looking and one 2- $\times$ 4- $\times$ 4-in up-looking NaI(Tl) scintillation detectors. Pulse inputs from the eight 2- $\times$ 4- $\times$ 16-in detectors were summed and recorded as a spectrum, as discussed in the following paragraphs. In addition, a spectrum from one of the 2- $\times$ 4- $\times$ 16-in detectors was recorded separately to provide increased dynamic range when viewing higher-radiation areas. Counts from the 2- $\times$ 4- $\times$ 4-in detector were recorded for possible use in correcting nonterrestrial radiation contributions. The 2- $\times$ 4- $\times$ 16-in detectors were surrounded by thermal insulating foam and shielded on the top and sides with 0.03-in (0.076-cm) cadmium and lead sheets. The 2- $\times$ 4- $\times$ 4-in detectors were shielded on the bottom and sides with the cadmium and lead sheets.

Spectral data were acquired and displayed in real time using specialized instrumentation that processes, stores, and displays spectral data. This system was

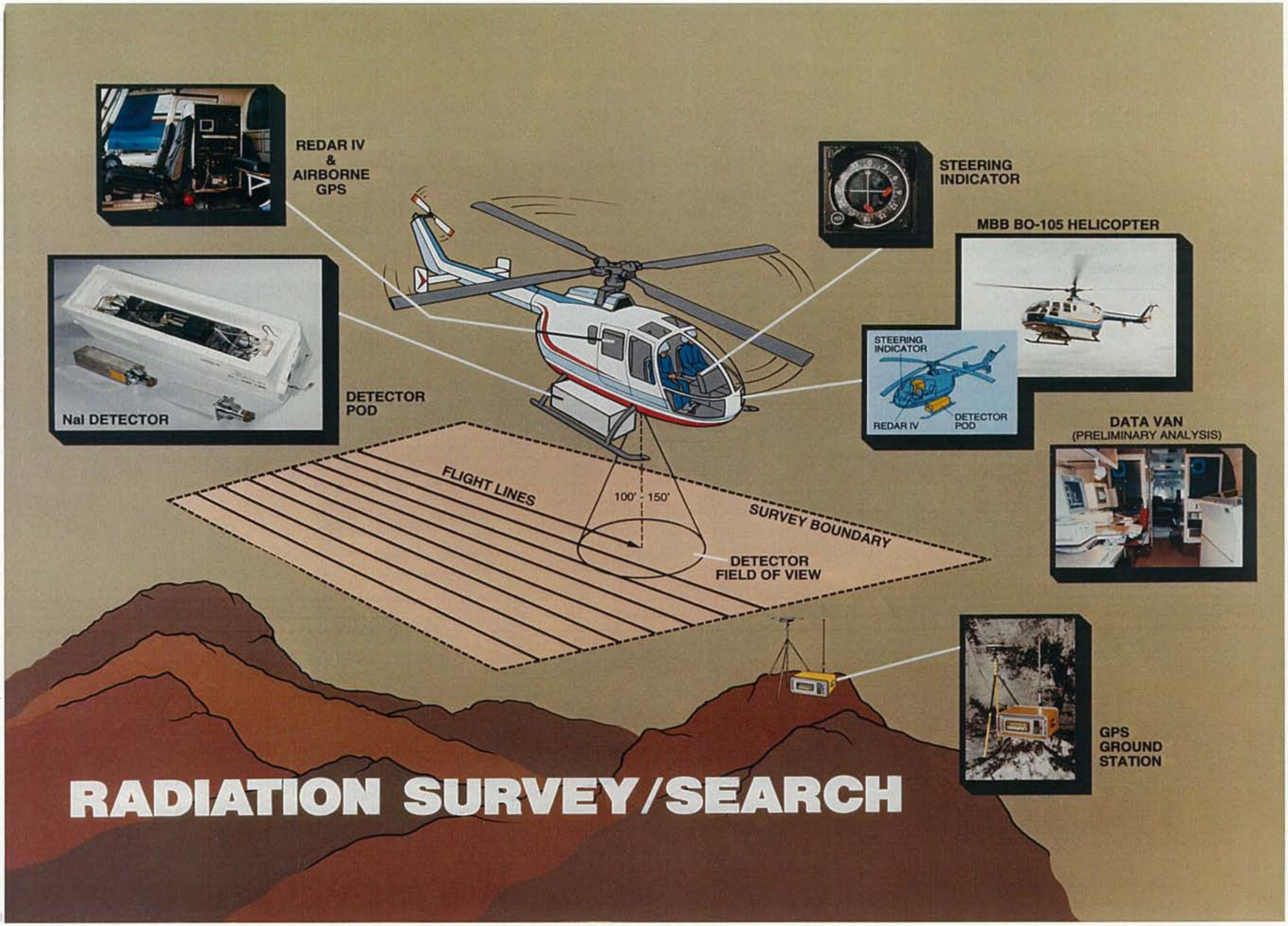

FIGURE 3. ***SURVEY DATA-ACQUISITION TECHNIQUE***

developed for aerial radiological surveys and contains the necessary instrumentation in a single package. The system, called the Radiation and Environmental Data Acquisition and Recorder, Version IV, (REDAR IV) system, is a multi-microprocessor and a portable data-acquisition and real-time analysis system.[4] It has been designed to operate in the severe environments associated with platforms such as helicopters, fixed-wing aircraft, and various ground-based vehicles. The system displays the required radiation and system information to the operator, in real time, through the display of a cathode-ray tube (CRT) and through multiple readouts. Pertinent data are recorded on cartridge tapes for later analysis.

The REDAR IV contains six subsystems: (a) two independent systems for collecting radiation data, (b) a general purpose data input/output (I/O) system, (c) a tape recording/playback system, (d) a CRT display system, (e) a real-time data-analysis system, and (f) a ranging system with steering calculation and display capabilities. These subsystems, which are under the operator's control, handle functions including data collection, analysis, and display; positional and steering calculations; and data recording.

Two multichannel analyzers (MCAs) in the REDAR IV system collect 1,024-channel, gamma-ray spectra (4.0 keV per channel) once every second during the surveying operation. The primary MCA (for the eight-detector spectrum) has a usable dynamic range of approximately 100,000 cps corresponding to an exposure rate at one meter AGL of about 1.5 mR/h. Spectral information at high-count rates begins to degrade at approximately half this rate; a single NaI(Tl) detector and second MCA are used when the system is used in high-count-rate situations.

The data-acquisition system is calibrated to a 0–4,000-keV energy range using gamma-ray sources of americium-241 (^{241}Am) at 60 keV, cobalt-60 (^{60}Co) at 1,173 and 1,332 keV, and cesium-137 (^{137}Cs) at 661 keV. A 28-keV, low-energy threshold is selected to minimize counts from the lower part of the continuum. The summed signal derived from the eight NaI(Tl) detectors was adjusted prior to processing by the analog-to-digital converter so that the calibration peaks appeared in preselected channels in the MCA of the data-acquisition system.

Because the energy resolution of NaI(Tl) crystals decreases with increasing energy, spectra are compressed to conserve storage space. Spectra are divided into three partitions where the detected photopeak width is approximately the same. Data in the first partition (0–300 keV) are not compressed to permit stripping of low-energy photopeaks such as the 60-keV photopeak from ^{241}Am. The second partition (300–1,620 keV) is compressed to 12 keV per channel while the third partition (1,620–4,000 keV) is compressed to 36 keV per channel. The spectral-compression technique reduces the amount of data storage required by a factor of four.

Two full spectra, one spectrum containing data from the eight detectors and a second spectrum containing data from a single detector, and related information such as position, time, and air temperature are continuously recorded every second. The REDAR IV system has two sets of spectral memories; each memory can accumulate four individual spectra. The two memories support continuous data accumulation: one memory stores data while the other memory transfers data to magnetic tape. At a survey speed of 70 knots (36 m/s), 45 data sets were acquired for each mile of flight. The Nine Mile Point/James FitzPatrick survey contained 40,000 data sets.

3.3 Detector Characteristics

The detector system was designed to sense terrestrial and airborne gamma radiation with energies between 20 and 4,000 keV. This energy range includes emitted gamma radiation from naturally occurring radionuclides and almost all man-made gamma radiation sources.

NaI(Tl) detectors used in this survey are characterized by their variable sensitivity versus incident gamma energy and by a footprint size that is also energy-dependent. The variation in sensitivity with incident energy is a well-known characteristic of NaI(Tl) detectors. Detailed data on detector sensitivity can be obtained from the manufacturer.[5] The dependence of the viewed footprint size with energy can be (approximately) modeled using Appendix B. Because of the large footprint, sources detected by aerial systems appear to be spread over a much larger area than would be indicated by ground-based measurements.

For uncollimated detectors such as those used in this aerial survey, the source-to-detector distance and the attenuation by the air effectively limit the viewed terrestrial area to a circular region centered beneath the detector. The size of the field of view is a function of the gamma-ray energy, the gamma-ray origin, and the detector response. Radionuclide activities on or in the soil and exposure rates normalized to one meter AGL are customarily reported but only as large-area averages. Activity, inferred from aerial data, for a source uniformly distributed over a large area compared to the field of view of the detectors is very good and generally agrees with ground-based measurements. However, activity for a point source, a line source, or a source activity less than the detector's field of view will be underestimated, sometimes by orders of magnitude. When this occurs, the aerial data simply serve to locate and identify such sources.

Apparent source-broadening makes comparison with ground-based measurements difficult. Radionuclides that occur as hot particles are averaged by the aerial detection system, appearing as uniform, large-area distributions. Ground surveys, however, would locate the hot particles within a smaller area and show the surrounding areas to be free of contamination. Table 2 contains estimates of the detection system's field of view or "footprint" size for several energies of interest.

Detector sensitivity is not constant throughout the footprint. The maximum sensitivity occurs directly beneath the detector; the sensitivity decreases with increasing horizontal distance between the source and airborne detector. Additionally, the incident gamma rays from even a monoenergetic source include scattered gamma rays once the incident radiation reaches the airborne detectors. Footprint sizes are, therefore, dependent on the source location: distributed in the soil, scattered by passing through air, shielded inside a container, etc.

4.0 DATA ANALYSIS

Data processing was initiated in the field using a computer analysis laboratory installed in a mobile van located near the survey site. Data were examined before leaving the site, and a preliminary analysis was completed to ensure that the raw data were satisfactory.

Standard techniques for analyzing survey data were used: terrestrial exposure rates were computed from gross count data with a correction for variations in altitude. Man-made radioactivity, ^{137}Cs, nitrogen-16 (^{16}N), and ^{60}Co, was determined through differences between total counts in appropriate spectral windows.[6]

Table 2. Approximate Detector Footprint Radius for Relative Count-Rate Contributions from Terrestrial Sources at a Survey Altitude of 150 ft (46 m)

Emitted Gamma-Ray Energy (keV)	Radius where 99% of Detected Counts Originate ft (m)	Radius where 90% of Detected Counts Originate ft (m)	Radius where 50% of Detected Counts Originate ft (m)
60	650 (198)	353 (108)	155 (47)
200	850 (259)	435 (133)	178 (54)
600	1,067 (325)	560 (171)	214 (65)
1,500	1,715 (523)	772 (235)	260 (79)
2,000	2,145 (654)	850 (259)	275 (84)
3,000	2,862 (872)	1,007 (307)	308 (94)
4,000	3,850 (1173)	1,150 (351)	322 (98)
6,000	4,295 (1309)	1,325 (404)	350 (107)

4.1 Natural Background Radiation

Natural background radiation originates from (a) radioactive elements present in the earth, (b) airborne radon, and (c) cosmic rays entering the earth's atmosphere. Natural terrestrial radiation levels depend on the types of soil and bedrock immediately below and surrounding the point of measurement. Within cities, the levels also depend on the nature of the pavement and building materials. The gamma radiation originates primarily from the uranium and thorium decay chains and from radioactive potassium. Local concentrations of these nuclides produce radiation levels at the surface of the earth typically ranging from 1–15 μR/h. Some areas having high concentrations of uranium and/or thorium in the surface minerals exhibit even higher-radiation levels, especially in the western states.[7] The peaks shown in Table 3 were found in the natural background spectrum. Figure 4 shows a typical spectrum from natural background radiation within the survey area.

Isotopes of the noble gas radon are members of both the uranium and thorium radioactive decay chains. Radon can diffuse through the soil and may travel through the air to other locations. Therefore, the level of airborne radiation due to these radon isotopes and their daughter products at a specific location depends on a variety of factors including meteorological conditions, mineral content of the soil, and soil permeability. Typically, airborne radon contributes 1–10 percent of the natural background radiation.

Cosmic rays interact with elements of the earth's atmosphere and soil. These interactions produce an additional natural source of gamma radiation. Radiation levels due to cosmic rays vary with altitude and geomagnetic latitude. Typically, values range from 3.3 μR/h at sea level in Florida to 12 μR/h at an altitude of 1.9 mi (3 km) in Colorado.[8]

4.2 Measured Terrestrial Exposure Rate

The measured count rate in the aircraft differs from the true terrestrial exposure rate due to background sources in the aircraft: (a) variation of cosmic radiation with altitude, (b) temporal variation in atmospheric radon concentrations, and (c) attenuation by the air of gamma rays emitted from the ground. Because the raw count-rate data over the survey area have been found to vary, the data from each flight were normalized to data that were measured over a test line at the beginning and end of each data-acquisition flight. This normalization was used to minimize the effects of variations in the natural airborne and background aircraft radiation. A test line west of the plant site, over farms and orchards, was selected for this survey.

Table 3. Gamma-Ray Photopeak Identifications—Background within the Survey Area

Energy (keV)	Identification
240	^{208}Tl (239 keV), ^{228}Ac (209 keV), ^{212}Pb (238 keV)
380	^{228}Ac (339 keV), ^{214}Bi (387 keV, 389 keV)
511 (weak)	^{208}Tl (511 keV), annihilation
610	^{214}Bi (609 keV)
830 (weak)	^{228}Ac (795 keV), ^{208}Tl (861 keV)
930	^{228}Ac (911 keV), ^{214}Bi (934 keV)
1,130	^{214}Bi (1,120 keV)
1,230	^{214}Bi (1,238 keV)
1,460	^{40}K (1,460 keV)
1,750	^{214}Bi (1,765 keV)
2,160	^{214}Bi (2,204 keV)
2,560	^{208}Tl (2,614 keV)

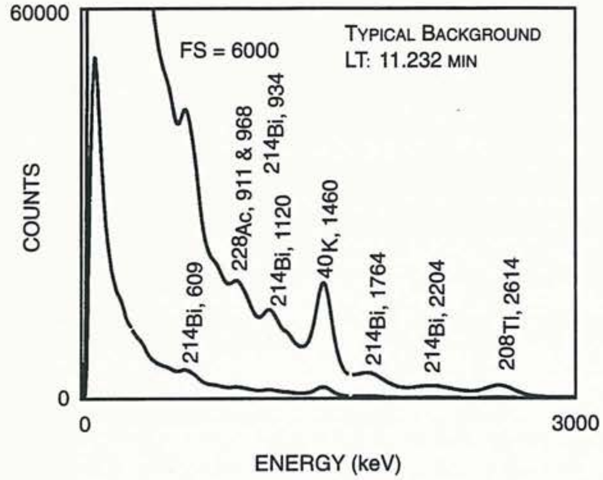

FIGURE 4. ***TYPICAL BACKGROUND SPECTRUM OF THE SURVEY AREA***

The terrestrial exposure rate can be calculated as follows:

$$Exposure\ \ Rate = (Conversion\ \ Factor)\ \ (GC - B)\ e^{-(A \cdot altitude)} \tag{1}$$

GC is the gross count rate (sum of the contents of all spectrum channels) recorded by the REDAR IV system, and A and B are constants. A is the site-specific, atmospheric attenuation coefficient and has been found to be constant over the duration of a survey. A is determined from data taken at multiple altitudes over the test line. B represents the nonterrestrial background count rate and is calculated from test-line count rates measured before and after each survey data flight (using the previously determined value of A). An average value of B, the recorded altitude at each data interval, and the value of A are used to correct all measurements to yield the correct terrestrial gamma-emission rate. (Such a correction could be gamma-ray energy-dependent. At present, it is assumed that the relative contributions to the measured spectrum do not vary between the test line and the survey area, so an average correction is appropriate.)

A three-point sliding interval average was applied to gross count-rate data to reduce statistical fluctuations in the data:

$$C_{i,avg} = (C_{i-1} + C_i + C_{i+1})/3 \tag{2}$$

$C_{i,avg}$ is the averaged value at the ith location, and C_{i-1}, C_i, and C_{i+1} are consecutive, corrected gross count rates along a single flight line. Present analysis codes do not average nearest-neighbor data on adjacent flight lines; three-point averaging has been found to be adequate. The exposure rate is calculated from this averaged gross count rate. Three-point sliding interval averaging was also applied to man-made and net isotopic data prior to calculating radiation contour maps.

The conversion factor, relating count rates to exposure rates, has been determined in several ways. It can be determined empirically by comparing ground-based, exposure-rate measurements with count rates from the airborne system. This was done for the Nine Mile Point/James FitzPatrick survey using data obtained from comparative ground-based and aerial measurements of a well-characterized reference line. Two reference lines are maintained for survey calibration: one in Calvert County, Maryland, and a second in the Lake Mohave National Recreation Area near Las Vegas, Nevada. Data from the Calvert County test line were used for the Nine Mile Point/James FitzPatrick survey because the Calvert County terrain is similar to the area covered by this survey. A conversion factor of 1.04×10^{-3} μR/h $(\text{cps})^{-1}$ was used in the Nine Mile Point/James FitzPatrick survey.[9,10]

This conversion factor and exposure rates that were calculated using the conversion factor are correct only in regions of natural background radiation. Rates in regions where the gamma-ray spectrum is dominated by man-made activity are useful as relative indicators. A reviewer of this report noted that the spectrum near the plant sites is significantly different from natural background due to the presence of gamma rays from ^{16}N.[11] Areas where ^{16}N was detectable are shown in Figure 5. Exposure-rate isopleths that lie beyond the area of detectable ^{16}N as shown in Figure 6 are most likely due to natural sources and are valid. Exposure-rate isopleths shown in regions of Figure 6 near the plant sites (areas of detectable ^{16}N) should be considered to be relative measurements.

The terrestrial exposure-rate isopleth plots are also used as a quality check on the systematic variability of survey data. In particular, exposure-rate isopleths that fall along flight lines, especially along the initial or

CONVERSION SCALE

LETTER LABEL	NITROGEN - 16 EXCESS COUNT RATE*
A	< 8
B	8 - 25
C	25 - 80
D	80 - 250
E	250 - 800
F	800 - 2,500
G	2,500 - 8,000
H	8,000 - 25,000
I	25,000 - 80,000

*Counts per second as observed at a 150-foot (46-meter) survey altitude in the gamma energy window of 2,702 keV and up.

FIGURE 5. *DISTRIBUTION OF ^{16}N WITHIN THE SURVEY SITE*

FIGURE 6. *TERRESTRIAL EXPOSURE RATES WITHIN THE SURVEY SITE*

final lines of individual flights, indicate instability in the detection system. Such variations must be corrected before the data are used. If they cannot be corrected, the uncertainty (error bars) applied to the isopleth plots must be increased to eliminate obvious systematic variations.

4.3 Identifying Sources of Man-Made Radiation from Aerial Survey Data

Contaminated sites are located from isopleth maps based on a man-made radiation source algorithm, referred to as the man-made gross count rate (MMGC). This analysis provides a general overview of contamination within the survey area and also indicates the areas that should be further investigated. The MMGC algorithm is based on several observations: (a) commonly occurring man-made sources emit gamma rays having energies less than 1,394 keV while natural background sources emit gamma rays both below and above this threshold and (b) the spectrum continuum shape is relatively constant throughout the survey area. Moreover, gamma rays detected after they are scattered (*i.e.*, emitted by sources buried in the soil or through atmospheric scattering) will contribute to the continuum at energies below their initial energies.

The measured spectral shape is constant over the survey area assuming (a) a stable cosmic-ray emission rate; (b) a constant background due to the aircraft, airborne radon, and natural sources; and (c) a survey area where the gamma sources and soil composition change slowly in relative comparison to the area contributing to the measured spectrum. Experience has shown that these assumptions are reasonable within statistical uncertainties over large, uncontaminated survey areas. (Significant changes in the source characteristics will invalidate this assumption. For example, changes in the MMGC are seen in spectra acquired over different terrain and when airborne radon levels change.)

If there were no systematic errors in the detection system, the sum of all gamma radiation due to man-made sources would be the difference between the spectrum in question and a typical background spectrum. Unfortunately, systematic errors make this simple subtraction impractical. A more reliable comparison can be made using the ratios of the sum of all channel contents of the spectral region from 38–1,394 keV (the region of man-made gamma emitters) to the sum of the spectral region from 1,394–3,026 keV (the region containing mostly counts from naturally occurring gamma emitters).

$$MMGC = \sum_{E=38\ \mathrm{keV}}^{1394\ \mathrm{keV}} C_i - \left[Normalization \cdot \sum_{E=1394\ \mathrm{keV}}^{3026\ \mathrm{keV}} C_i \right] \tag{3}$$

C_i represents the contents of spectrum channels corresponding to energies within the range of summation. The MMGC is the difference for a spectrum measured over an area containing man-made radionuclides, computed using the previously determined normalization constant. The constant is computed from data measured over areas free of contamination as follows:

$$Normalization\ \ Constant = \frac{\sum_{E=38\ \mathrm{keV}}^{1394\ \mathrm{keV}} C_i}{\sum_{E=1394\ \mathrm{keV}}^{3026\ \mathrm{keV}} C_i} \tag{4}$$

The normalization constant is derived from the data of each flight to minimize the effects of airborne radon-222 (^{222}Rn) and minor system characterization differences between flights.

Detected high-energy gamma rays, such as the 6.13-MeV gamma ray emitted by ^{16}N, interfere with the MMGC computation: the contribution to the Compton continuum due to high-energy gamma rays contributes to the total spectrum over a broad range of energies below the photopeak. This contribution changes the spectral shape, invalidating the assumption used to calculate the normalization constant.

4.4 Isotope-Specific Information from Aerial Survey Data

While the MMGC provides an indication of radioactive contamination, nuclide-specific information is important for such activities as identifying contamination sources and site remediation. Aerial survey data are also examined for spectral peaks due to various radionuclides that could reasonably be expected at the survey site: ^{60}Co and ^{137}Cs. Annihilation radiation at 511 keV was also examined as this line was prominent in previous survey data from boiling-water reactor sites.[12] The 511-keV gamma rays are generated from pair production resulting from the interaction of the 6.13-MeV ^{16}N gamma rays with materials. Nitrogen-16 is normally produced in the steam cycle of boiling-water reactors from an (n,p) reaction on oxygen-16 (^{16}O).

Spectral-stripping techniques were used to analyze aerial radiation data. (Peak fitting is not used because peak shapes from the NaI[Tl] detectors are broad and frequently overlap.) Spectra from areas of interest (usually those with significant MMGC levels) are analyzed by subtracting, channel-by-channel, a spectrum of a known background area. These spectra are sums of all spectral data acquired within the area:

$$Difference\ \ Spectrum_i = C_{i,site\ of\ interest} - K_{diff} \cdot C_{i,background} \tag{5}$$

The K_{diff} constant is selected to force the difference spectrum to zero at the high-energy side. Spectral peaks are readily visible in the difference spectrum. The presence of an identifiable spectral peak is considered to be a requirement for proceeding with isotopic isopleth plots. Once identified, contour plots of individual radionuclides are computed using two- or three-window spectral-stripping techniques on each data spectrum acquired during the survey as follows:

$$Isotopic\ \ Net\ \ Count = \sum_{E=E_1}^{E_2} C(E) - (Scaling\ \ Factor) \cdot \left[\sum_{E=E_3}^{E_4} C(E) + \sum_{E=E_5}^{E_6} C(E) \right] \tag{6}$$

$C(E)$ represents the spectrum channel contents, and E_I represents the limiting energy ranges of the windows. This technique is shown graphically in Figure 7. Again, the scaling factor is adjusted to set the isotopic net count to zero for data from known background regions. Spectral window ranges used for isotopic data presented in this report are shown in Table 4.

Nitrogen-16, which is present near operating boiling-water reactors, emits an intense gamma ray at 6.13 MeV. This gamma peak is not seen in the spectrum, but the REDAR IV system records the presence of this gamma ray by storing all detected gamma counts above 4.0 MeV in the last spectrum channel. An estimate of the extent of ^{16}N around the plant site can be computed from the contents of the highest spectral channel and the continuum above 2,614 keV:

$$Net(^{16}N) = \sum_{E=2750\ \mathrm{keV}}^{4000\ \mathrm{keV}} C_i + C_{E>4000\ \mathrm{KeV}} - B \tag{7}$$

$C_{E>4000\ keV}$ is the sum of all detected gamma rays above 4.0 MeV, and B is a constant. A value of 9.0 was selected for B by assuming that the ^{16}N count rate far from the plant site was zero.

Nuclide-specific conversion factors take into consideration the isotopic-branching ratios, the spectral window analysis, and an assumed distribution of the

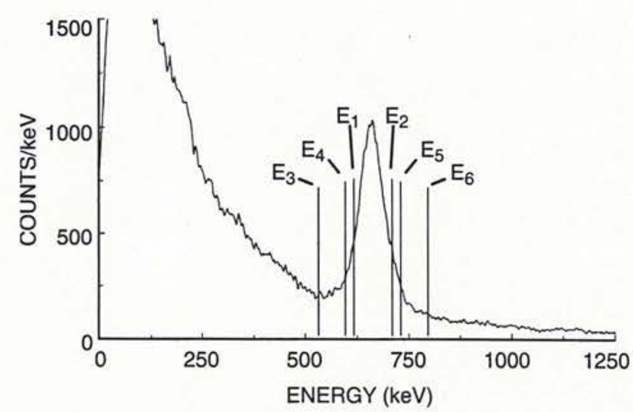

FIGURE 7. *SPECTRAL WINDOW EXTRACTION EXAMPLE*

Table 4. Spectral Regions Used in Net Isotopic Count-Rate Calculations

Isotope	Peak Region (keV)	First Background Region (keV)	Second Background Region (keV)
^{137}Cs	590 – 734	506 – 590	734 – 794
^{60}Co	1,094 – 1,394	1,394 – 3,026	
^{16}N	2,750 – 4,000		

source in the soil. The assumed distribution and soil attenuation at the gamma-ray energy being analyzed clearly affect the calibration. An assumed distribution of radionuclides is often a best estimate leading to an unavoidable uncertainty in the computed soil activity. Contamination may be dispersed on the surface with no contamination below the surface, or it may be distributed throughout the soil. The latter case has been found to be more probable. For the Nine Mile Point/James FitzPatrick survey, an exponential distribution was assumed based on actual depth profile measurements of similar radionuclides.[13] Calculation of conversion factors based on these distributions is discussed in Appendix B.

4.5 Detection Limits

Aerial radiological survey results provide information about radiation levels at the nuclear power plant site (generally above background) and in the surrounding area (generally a relatively constant background). Higher levels of radiation within the plant site are expected; the plant operator usually has ground-based measurements of the site. Aerial radiological survey data provide a check on the extent of higher levels of radiation near the site. Due to the large survey footprint, aerial data are only an approximate measure of the extent of site-based radioactivity. There are less costly means than aerial radiological surveys to determine that the exposure rate (ground-based radioactivity, etc.) within the site boundary of a nuclear power plant is greater than the exposure rate of the surrounding countryside.

Radioactivity in the off-site area surrounding the plant, especially from plant site emissions, is assumed to consist of large areas (compared to the survey detection footprint) of natural and man-made radioactivity. The surrounding area is too large (and possibly inaccessible) for ground-based measurements and is best examined using aerial survey data. Man-made radioactivity from plumes of material emitted from the plant site is of interest. Activity outside the boundary of the plant site will likely be much less than activity inside the plant site boundaries. Detection limits used in analyzing the Nine Mile Point/James FitzPatrick survey data were established to identify the lowest practical off-site contamination levels.

Aerial radiological survey data consist of many single measurements distributed over the survey area. It has been found from previous surveys that the survey data always contain large regions of background radiation with a few anomalous locations (*i.e.*, the reactor site). Knowing this, the survey data can be treated as a single, large data set for isotopic net counts and MMGC. The Nine Mile Point/James FitzPatrick survey data contained approximately 40,000 observations, a population sufficiently large that statistical analysis can be applied. Specifically, detection limits (minimum detectable activities) can be estimated using methods similar to those developed by Currie.[14] The following discussion can be applied to both MMGC and isotopic net count rates.

Currie defines two limits that are useful in analyzing survey data: (a) a critical level which is the minimum count rate where one would assume that data from a footprint are different from the background in the survey area and (b) a detection limit which is the minimum activity source that can reliably be detected. The critical level, L_C, is determined by considering the distribution of count rates in the background data set (generally the survey area outside the immediate reactor site) such that a fraction of all measured (calculated) quantities in the background data are less than or equal to L_C. This level addresses "type 1 errors" (failures to detect anomalous data). If a measurement or group of measurements is above L_C, then this region of the survey requires further examination. L_C is expressed as follows:

$$L_C = k \cdot \sigma \tag{8}$$

The value of σ is determined from the distribution of survey data. The value of k is selected based on the integral of a normal distribution from minus infinity to L_C such that a desired fraction (*e.g.*, 99.9 percent) of the observations in the distribution of background data is less than L_C, assuming normally distributed data. Examination of actual distributions of survey data supports this assumption. A measured value exceeding L_C would be assumed to indicate radiation above background within a specified confidence level.

L_C should not be considered a dimensioned quantity. Individually measured and/or computed values would be distributed around the "real" value (mean value). A single, measured observation equal to L_C could arise from measuring a range of "actual" activity levels.

The detection limit, L_D, may be understood by considering a single measurement of one survey footprint. Multiple measurements of this footprint would yield a distribution of values with a centroid corresponding to the actual (mean) activity within the footprint. Assuming a normal distribution of measurement values, Currie defines L_D as the minimum activity (centroid of the distribution of measurements) where a desired fraction of all single measurements will fall above L_C:

$$L_D = 2\ L_C + k^2 \tag{9}$$

Equation 9 is based on Currie's analysis for radiation-counting data (Poisson statistics). For example, greater than 99.9 percent of all measured and/or calculated values for any "detectable" source (whose activity is L_D or greater) will be above L_C. The desired fraction (or percentage) of the cumulative distribution of observations is commonly referred to as the *confidence level*. This ensures that a source whose activity is equal to or greater than L_D will "always" be detected. L_D represents the lowest-activity level that the survey detection process will consistently find.

The lowest-radiation isopleth level in a typical contour plot would be set at (or near) L_C while L_D would be the stated minimum detectable activity. (Higher contours are customarily defined in terms of "levels per decade," leading to an approximate logarithmic scale.) Radionuclide activities determined from net count values that are greater than L_C but less than L_D are reported although they are below the "detection limit" of the instrumentation.

Figure 8 shows the distribution of calculated MMGC values from the Nine Mile Point/James FitzPatrick survey data after applying sliding interval averaging. This distribution deviates from a true normal distribution, but a usable statistical uncertainty equal to 256 was calculated assuming a normal distribution. Isotopic net count rates of ^{137}Cs, ^{16}N, and ^{60}Co were normally distributed around zero.

Empirically determined L_C and L_D values for the Nine Mile Point/James FitzPatrick survey were obtained from examining the distribution of data. Table 5 shows the levels obtained from the survey data for 99.5 and 99.9 percent confidence levels. L_D values refer to radioactive material uniformly distributed on the surface (µCi/m^2), uniformly distributed throughout the soil versus depth (pCi/g[u]), or exponentially distributed throughout the soil versus depth (pCi/g[e]).

The previous analysis provides a rigorous means to estimate trip levels and minimum detectable activity levels for the Nine Mile Point/James FitzPatrick survey data. Unfortunately, application of statistical techniques leads to a problem of outliers. For example,

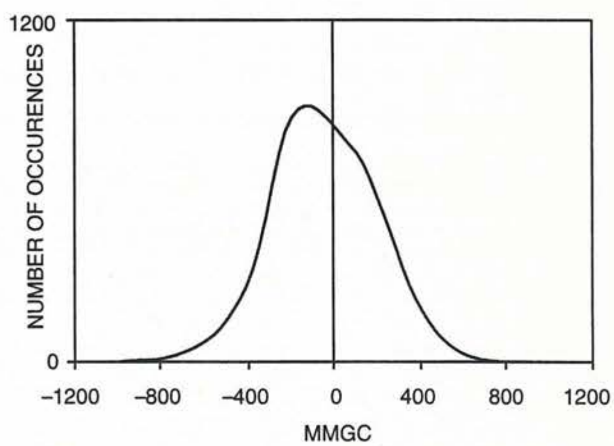

FIGURE 8. ***DISTRIBUTION OF MAN-MADE RADIATION DATA***

Table 5. Empirically Determined Detection Limits

Radionuclide	Statistical Uncertainty ($\sigma_{survey\ data}$)	Critical Level (L_C) 99.5% Confidence Level[a]	Critical Level (L_C) 99.9% Confidence Level	Detection Limit (L_D) 99.5% Confidence Level	Detection Limit (L_D) 99.9% Confidence Level
MMGC	256	658 net cps	794 net cps	1322 net cps	1597 net cps
^{60}Co	9.56	25 net cps	30 net cps	0.027 μCi/m^2 0.27 pCi/g (u)[b] 0.64 pCi/g (e)[c]	0.032 μCi/m^2 0.32 pCi/g (u) 0.74 pCi/g (e)
^{16}N[d]	2.36	6.06 net cps	7.30 net cps	18 net cps^2	23 net cps
^{137}Cs	13.3	34 net cps	41 net cps	0.064 μCi/m^2 0.82 pCi/g (u) 1.6 pCi/g (e)	0.075 μCi/m^2 0.97 pCi/g (u) 1.9 pCi/g (e)

[a] Confidence level as defined in the text.
[b] A uniform distribution of radioactive material versus depth throughout the soil.
[c] An exponential distribution of radioactive material having a relaxation length of 3 cm was assumed. The stated value is an average over the first 2.5 cm.
[d] ^{16}N is assumed to be a point source. No conversion factor is available to relate net cps to concentration.

basing L_C on a 99.5 percent confidence level will ensure that 99.5 percent of measurements from background areas (assumed to be free of man-made radiation) will fall below L_C, and 0.5 percent of all background-area data will be above L_C, leading to an erroneous conclusion that 0.5 percent of the total survey area is contaminated. For a set of 40,000 observations, 0.5 percent represents 200 survey footprint measurements.

One solution to the outlier problem is setting L_C at a value well above the background distribution but below the highest level seen over the nuclear power plant site. This approach has been used in the past, but the resulting large increase in minimum detectable activity would fail to detect low-level contamination. Another method deals with outliers by requiring spatial correlations between data of minimal activity. Here it is assumed that individually measured values near L_C are outliers if the data nearest the value in question were below L_C. Data values much higher than L_C do not require spatial correlations to be valid.

The Nine Mile Point/James FitzPatrick survey radiation isopleth plots using L_C values, based on 95, 99, 99.5, and 99.9 percent confidence levels, were examined for spatial correlations. Confidence-level plots of 95 and 99 percent contained many outliers and were judged not to be useful. Plots containing both 99.5 and 99.9 percent confidence-level contours were examined, and it was found that both levels yielded essentially identical features with the 99.5 percent confidence-level plot containing numerous one-footprint "contours" that were judged to be statistical outliers.

The 99.9 percent confidence level was selected as the lowest-contour level presented on the Nine Mile Point/James FitzPatrick isopleth plots. The probability that two adjacent data measured on two different flight lines are both outliers is $(0.001)^2 = 1 \times 10^{-6}$.

It is also possible to determine L_C and L_D from model calculations. Such calculations are useful in planning survey operations. Appendix B contains a table of predicted critical levels and detection limits for conditions similar to those of the Nine Mile Point/James FitzPatrick survey.

5.0 AERIAL RADIOLOGICAL SURVEY RESULTS

Radiation isopleth plots were made of the Nine Mile Point/James FitzPatrick site for exposure rate, MMGC, ^{137}Cs, ^{16}N, and ^{60}Co. Of these, exposure rate, MMGC, and ^{16}N are presented in this report. The

^{60}Co and ^{137}Cs plots showed activity only around the plant site, as expected, and showed no activity in the remainder of the survey area.

5.1 Terrestrial Exposure Rates

Figure 6 is a plot of the terrestrial exposure rates near the Nine Mile Point/James FitzPatrick plant site. The contribution from cosmic rays and airborne radon was included. Minimum exposure rates are detected over water; exposure over land varies within a small range depending on the terrain. These correlate with differences in the terrain, which are visible on the aerial photo. The highest rate was seen over the Nine Mile Point and James FitzPatrick Plant sites, as expected. There were no other areas with comparable exposure rates in the surrounding survey area. The large bullseyes around the plant site result from broadening effects discussed previously; the actual higher-exposure-rate area was smaller than it appears.

Three ground-based, exposure-rate measurement locations are shown on the exposure-rate plot. These were acquired using a calibrated, pressurized ion chamber.* Ground-based and aerial survey exposure rates are compared in Table 6.

Exposure rates calculated from the aerial survey data were consistently higher than those determined from ground-based data. These differences can be attributed to the smaller footprint of the pressurized ion chamber, variations in the spectrum at the site, a smaller than expected cosmic-ray contribution, differences in radon concentration (the aerial and ground measurements were made on different days), and measurement uncertainties in the aerial detection systems.

* Reuter-Stokes, Model RSS-112, calibrated by the manufacturer.

5.2 Man-Made Gross Count Rates

MMGC contours for the Nine Mile Point/James FitzPatrick survey are shown in Figure 9. The plot shows the 99.9 percent confidence level and higher rates. No useful data were available over the cross-hatched region due to distortion of the spectral shape in the region of high ^{16}N gross count rates. Otherwise, the MMGC plot shows remarkably little activity within the survey area.

5.3 Isotopic Data

Evidence of man-made and naturally occurring gamma emitters was found in the Nine Mile Point/James FitzPatrick survey area. Figure 5 shows the distribution of ^{16}N where the lowest-level contour corresponds to a 99.9 percent confidence level. The highest levels of ^{16}N are centered over the Nine Mile Point and James FitzPatrick reactor sites with measurable levels extending approximately 0.5 mi from each plant. It was initially believed that these results indicated an ^{16}N release from both reactor sites due to the large area where ^{16}N was detected.

Monte Carlo photon transport calculations were used to predict expected contour maps for both point and dispersed ^{16}N sources.[15] (The "point source" was a

Table 6. Comparison of Ground-Based (Pressurized Ionization Chamber) and Aerial Survey Exposure Rates (Cosmic[a] plus Terrestrial)

Point Number	Location	Exposure Rate (μR/h) ± 1 Standard Deviation: Ground-Based Measurement	Aerial Survey Measurement
1	North Scriba, County Route 29	6.9 ± 0.3	7.8 ± 0.3
2	Lakeview Road	6.8 ± 0.2	7.6 ± 0.3
3	Test line, Route 51 South	7.7 ± 0.3	8.3 ± 0.3

[a] The cosmic contribution is assumed to be 3.6 μR/h.

FIGURE 9. *MAN-MADE RADIATION WITHIN THE SURVEY SITE*

half cylinder, 30 ft in diameter by 50 ft long; the "dispersed"source was a large square. A realisticallysized NaI(Tl) detector was included also.) The results of point-source modeling show a sharply peaked relative intensity versus distance from the source, increasing from a relative magnitude of unity at a 1.3-mi radius to a relative level of 10^6 at a 1,000-ft radius. Modeling results for a dispersed source predict a more gradual increase over an approximate 3,000-ft distance from the edge of the plume. In addition, the results of point-source modeling show circular contours while the dispersed source contours follow the shape of the dispersed plume. The ^{16}N contour data resemble the results of point-source modeling; the center area "H" and "I" level contours represent intensities of 3.5 and 4 orders of magnitude, respectively, higher than the lowest-detectable level. A superposition of radiation emitted from two adjacent boiling-water reactor sites is readily apparent. The extent of these highest-level contours is approximately 600-ft-diameter circles over each site. It appears that the large-area detectable ^{16}N levels resulted from intense, contained ^{16}N sources at the plant sites. There are no other areas of measurable ^{16}N within the survey boundary.

Examination of ^{137}Cs and ^{60}Co isopleth plots showed no detectable activity within the survey area although these radionuclides were detected on close examination of spectra over the plant sites. Figure 10 contains spectra from areas of interest: Spectrum A is a sum of the spectra over the Nine Mile Point site while Spectrum B is a sum of the spectra from above a higher-exposure-rate area over the James FitzPatrick site.

Table 7 lists the gamma-ray photopeak energies present in Spectrum A with the probable radioisotopic identifications. Spectrum A contains peaks due to ^{60}Co and naturally occurring gamma emitters: ^{214}Bi, ^{228}Ac, and ^{208}Tl. Spectral features have been broadened due to the higher ^{16}N count rates.

Table 8 lists the gamma-ray photopeak energies present in Spectrum B with the probable radioisotopic identifications. Spectrum B contains peaks due to a multitude of probable and possible man-made emitters and naturally occurring gamma emitters. Some of the weak peaks were identified by stripping a background spectrum from the spectrum measured over the area of interest. Weak peaks should be considered "possible" due to the quality of spectra available from NaI(Tl) detectors.

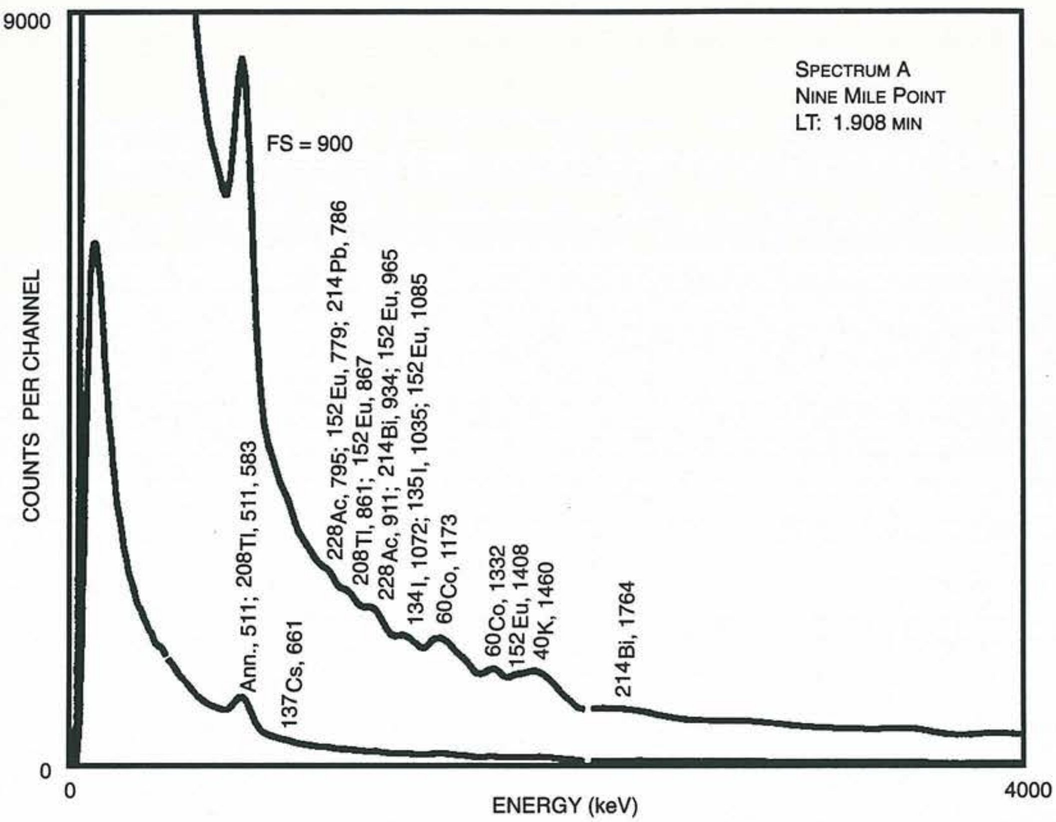

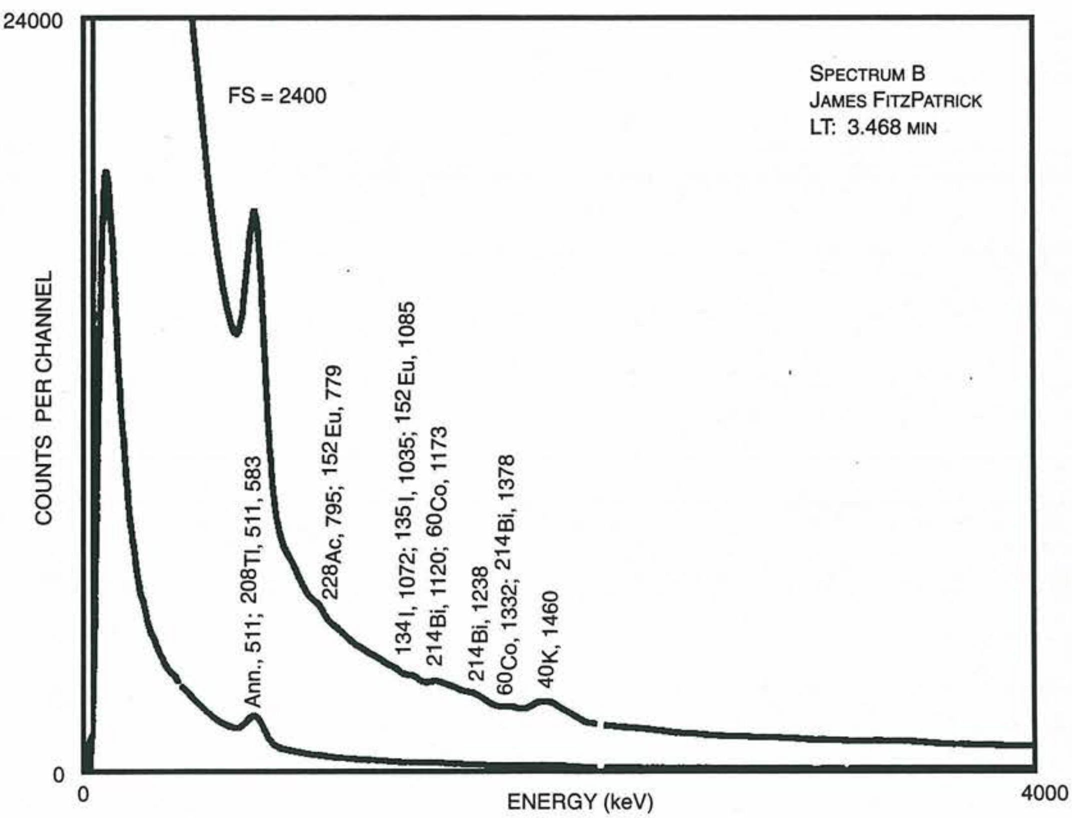

FIGURE 10. ***SPECTRA OF AREAS OF INTEREST***

Table 7. Probable Gamma-Ray Photopeak Identifications—Spectrum A (Above the Nine Mile Point Reactor)

Energy (keV)	Identification
530	^{208}Tl (511, 583 keV), annihilation (511 keV)
670 (weak)	^{137}Cs (662)
810 (weak)	^{214}Pb (786 keV), ^{228}Ac (795 keV), ^{152}Eu (779 keV)
880 (weak)	^{208}Tl (861 keV), ^{152}Eu (867 keV)
940	^{214}Bi (934 keV), ^{228}Ac (911 keV), ^{152}Eu (965 keV)
1,060	^{152}Eu (1,085 keV)
1,160	^{60}Co (1,173 keV), ^{214}Bi (1,120 keV), ^{65}Zn (1,115 keV)
1,220	^{214}Bi (1,238 keV)
1,320	^{60}Co (1,332 keV)
1,410	^{152}Eu (1,408 keV)
1,460	^{40}K (1,460 keV)
1,760 (broad)	^{214}Bi (1,765 keV)
2,550 (broad, weak)	^{208}Tl (2,614 keV)

Table 8. Gamma-Ray Photopeak Identifications—Spectrum B (Above the James FitzPatrick Reactor)

Energy (keV)	Identification
540	^{208}Tl (511, 583 keV), annihilation (511 keV)
620 (weak)	^{214}Bi (609 keV), ^{134}I (595 keV)
660 (weak)	^{137}Cs (662)
760 (weak)	^{228}Ac (795 keV), ^{152}Eu (779 keV)
790 (weak)	^{214}Pb (786 keV), ^{228}Ac (795 keV), ^{152}Eu (779 keV)
860 (weak)	^{208}Tl (861 keV), ^{152}Eu (867 keV)
940 (weak)	^{214}Bi (934 keV), ^{228}Ac (911 keV), ^{152}Eu (965 keV)
1,040 (weak)	^{152}Eu (1,085 keV)
1,140 (weak)	^{60}Co (1,173 keV), ^{214}Bi (1,120 keV) ^{65}Zn (1,115 keV)
1,220 (weak)	^{214}Bi (1,238 keV)
1,300 (weak)	^{60}Co (1,332 keV)
1,410 (weak)	^{152}Eu (1,408 keV)
1,460	^{40}K (1,460 keV)
1,760 (weak)	^{214}Bi (1,765 keV)
2,560 (broad, weak)	^{208}Tl (2,614 keV)

APPENDIX A

SURVEY PARAMETERS

Survey Site:	Nine Mile Point and James FitzPatrick Nuclear Power Plants
Survey Location	Lycoming, New York
Survey Date:	October 12–17, 1995
Survey Coverage:	9.1 sq mi (23.6 sq km)
Survey Altitude:	150 ft (46 m)
Aircraft Speed:	70 knots (36 m/s)
Line Spacing:	250 ft (76 m)
Line Length:	Flight lines varied in length from 1–6 miles
Line Direction:	North–South
Number of Lines:	Approximately 127
Detector Array:	Eight (2- × 4- × 16-in) NaI(Tl) detectors Two (2- × 4- × 4-in) NaI(Tl) detectors
Acquisition System:	REDAR IV
Aircraft:	MBB BO-105 helicopter (Tail Number N40EG)
Project Scientist:	A.E. Proctor

APPENDIX B

DERIVATION OF CONVERSION FACTORS

The relationship between the photopeak net-count rate observed at a distance, h, above the surface and the activity of a monoenergetic gamma emitter distributed in the soil can be written as follows:[16,17]

$$\phi = \int_0^{\infty}\int_0^{\infty} \frac{S_V(z)}{4\pi D^2}\; e^{-\left(\frac{\mu}{\rho}\right)_a \rho_a r_a}\; e^{-\left(\frac{\mu}{\rho}\right)_s \rho_s r_s}$$

$$2\pi x \; dx \; dz \qquad \text{(B-1)}$$

where

ϕ = photopeak flux at the detector

$S_V(z)$ = activity per unit volume; usually assumed to be a function of depth in the soil ([γ/s]/cm^3)

D = detector-to-source distance in the air and the soil combined (cm); $r_a + rs$

z = source distribution depth in the soil (cm)

x = integration variable;

$$D = \left[x^2 + (h+z)^2\right]^{1/2}$$

$(\mu/\rho)_a, (\mu/\rho)_s$ = air and soil mass attenuation coefficients for the monoenergetic gamma energy (cm^2/g)

ρ_a, ρ_s = air and soil density (g/cm^3)

For man-made radioactive material distribution patterns, the distribution of a gamma emitter in the soil can be approximated by an exponential vertical distribution of concentration:

$$S_V(z) = S_{V0}\; e^{-az} \qquad \text{(B-2)}$$

S_{V0} is the activity per gram of soil at the surface, and α is the reciprocal of the relaxation depth. This implies that the representative volume of soil at a relaxation depth of $1/\alpha$ contains approximately 63 percent of the source's total activity. At relaxation depths of $2/\alpha$ and $3/\alpha$, the representative volume of soil contains approximately 86 and 95 percent, respectively, of the total activity.

The effective area, A, represents the detector's capability or efficiency in detecting the specific gamma ray:

$$N_p = A \;\; \phi \qquad \text{(B-3)}$$

N_p is the photopeak net count rate, and ϕ is the incident flux on the detector. The effective area, in general, varies as a function of the gamma-ray angle incident to the detector face and can be written as follows:

$$A = A_0 R(\theta) \qquad \text{(B-4)}$$

A_0 is the detector-effective area for a unit flux perpendicular to the detector face (zero degrees) (cm^2). $R(\theta)$ is the ratio of the detector response at an angle θ to its response at zero degrees. In practice, the effective area is measured with point radiation sources of different energies whose activities are traceable to the National Institute of Science and Technology.

Rewriting Equation B-1 in terms of θ and z and combining Equation B-4 leads to an expression which relates the measured photopeak count rate to the source activity where the conversion factor can be expressed in units of cps/(γ/cm^3-s).

$$\frac{(Np)}{S_{V0}} = \frac{A_0}{2}\int_0^{\frac{\pi}{2}} R(\theta)\tan\theta \frac{e^{-\left(\frac{\mu}{\rho}\right)_a \rho_a h \sec\theta}}{\alpha + \left(\frac{\mu}{\rho}\right)_s \rho_s \sec\theta}\, d\theta \qquad \text{(B-5)}$$

For a specific isotope, the conversion factor can be changed to units of cps/(pCi/cm^3) by converting gamma rays per second into pCi. This conversion depends on the branching ratio, β, which is the number of gamma rays emitted per disintegration. Multiplying the expression in Equation B-5 by the soil density (g/cm^3), the conversion factor can be given in units of cps/(pCi/g).

The average radionuclide concentration in the top z cm in the soil can be written for an exponentially distributed gamma emitter as follows:

$$S_V^z = \frac{1}{z}\int_0^z S_{V0}\ e^{-\alpha z}dz = \frac{S_{V0}}{\alpha z}\ (1 - e^{-\alpha z}) \qquad \text{(B-6)}$$

By substituting Equation B-6 into Equation B-5 and dividing by the soil density, the conversion factor can be expressed in units of (pCi/g)/cps as follows:

$$\frac{\left(\frac{S_V^z}{\rho_s}\right)}{N_p} = \frac{(1 - e^{-\alpha z})}{\alpha\ z}\ \beta \left[\frac{A_0\ \rho_s}{2}\int_0^{\frac{\pi}{2}} R(\theta)\tan\theta \frac{e^{-\left(\frac{\mu}{\rho}\right)_a \rho_a h\ \sec\theta}}{\alpha + \left(\frac{\mu}{\rho}\right)_s \rho_s\ \sec\theta} d\theta\right]^{-1}$$

(B-7)

Examples of computed minimum detectable activities and conversion factors for soil concentration from point radiation sources can be found in the literature.[18,19]

Estimated conversion factors can be computed for specific survey conditions through numerical integration of the previous equation. Combining these conversion factors with representative spectral background count rates and calculating Currie's detection limits yield dimensioned values of the detection limits. The limits shown in Table B-1 have been calculated for the Nine Mile Point/James FitzPatrick survey using the Calvert County, Maryland, reference line as the spectral background.

Table B-1. Calculated Critical Levels and Minimum Detectable Activity Versus Energy for Isotopic Analysis Based on a Realistic Background Spectrum

Assumptions: 70-knot airspeed, 150-ft survey altitude, 2.5-cm sample averaging depth, 3-cm relaxation depth, unity branching ratio, unity spectral-window factor, and 95 percent confidence level. [a]

	Net Spectral Window Count Rates		Minimum Detectable Activity (L_D)				
			Point Source		Distributed Source		
Energy (keV)	Critical Level (L_C)	Minimum Detectable Activity (L_D)	Directly Beneath the Detector (mCi)	Beneath the Detector Offset by 75 ft (23 m) (mCi)	Uniform Distribution Versus Depth (pCi/g)	Exponential Distribution Versus Depth (pCi/g)	Uniformly Distributed on the Surface ($\mu Ci/m^2$)
60	36	75	0.583	0.856	2.92	3.29	0.0829
200	48	100	0.467	0.662	1.03	1.57	0.0545
600	36	75	0.535	0.736	0.671	1.27	0.0505
1,500	23	48	0.603	0.816	0.431	1.05	0.0466
2,000	16	34	0.570	0.767	0.341	0.905	0.0414
3,000	4	11	0.301	0.402	0.139	0.422	0.0200

[a] "Confidence level" as defined in Section 4.5.

REFERENCES

1. *Radiological Survey of the Area Surrounding the Nine Mile Point Nuclear Station, Scriba, New York.* Report No. EGG-1183-1592, 1973; EG&G, Las Vegas, Nevada.

2. Boyns, P. K. *An Aerial Radiological Survey of the Area Surrounding the Nine Mile Point Nuclear Power Station, Scriba, New York.* Report No. EGG-1183-1656, 1977; EG&G, Las Vegas, Nevada.

3. Jobst, J.E. "Recent Advances in Airborne Radiometric Technology," *Remote Sensing Technology, Proceedings of a Symposium on Remote Sensing Technology in Support of the United States Department of Energy, 23–25 February 1983*. Report No. EGG-10282-1057, 1985; EG&G/EM, Las Vegas, Nevada.

4. *Radiation, Environmental Data Acquisition and Recorder System (REDAR IV) Manual.* 1981; Aerial Measurement Operations, EG&G, Las Vegas, Nevada.

5. Belian, J.; R. Dayton. *NaI(Tl) Scintillation Detectors.* Bicron Corporation.

6. Hendricks, T.J. "Radiation and Environmental Data Analysis Computer (REDAC) Hardware, Software, and Analysis Procedures," *Remote Sensing Technology Proceedings of a Symposium on Remote Sensing Technology in Support of the United States Department of Energy, 23–25 February 1983.* Report No. EGG-10282-1057, 1985; EG&G/EM, Las Vegas, Nevada.

7. Lindeken, C.L.; K.R. Peterson; D.E. Jones; R.E. McMillen. "Geographical Variations in Environmental Radiation Background in the United States," *Proceedings of the Second International Symposium on the Natural Radiation Environment, August 7-11, 1972, Houston, Texas.* National Technical Information Service, 1972; pp 317-332. Springfield, Virgina.

8. Klement, Jr., A.W.; C.R. Miller; R.P. Minx; B. Shleien. *Estimates of Ionizing Radiation Doses in the United States, 1960-2000.* U.S. EPA Report ORP/CSD72-1, 1972; EPA, Washington, D.C.

9. Proctor, A.E. [Oral communication with M.F. Mohar, Washington Aerial Measurments Organization, Andrews Air Force Base]. 1995 October.

10. Mohr, R.A. *Ground Truth Measurements at the Calvert County, Maryland Test Line*. Report No. EGG-10282-2066. 1985; EG&G/EM, Santa Barbara, California.

11. Proctor, A.E. [Oral communication with G.D. Baker, Niagra Mohawk Power Corporation]. 1997 January.

12. Maurer, R. *An Aerial Radiological Survey of the Quad Cities Nuclear Power Station and Surrounding Area*. Report No. EGG-10617-1219, 1993; EG&G/EM, Las Vegas, Nevada.

13. Essington, E.H.; E.B. Fowler. "Distribution of Transuranic Radionuclides in Soils, A Review," *Transuranics in Natural Environments, A Symposium at Gatlinburg, October 1976*. NVO-178, 1977; pp 41-77.

14. Currie, L.A. "Limits for Qualitative Detection and Quantitative Determination; Application to Radiochemistry." *Analytical Chemistry 40*. 3:586-593; 1968.

15. Proctor, A.E. [Oral communication with L. Tunnel]. 1997 January.

16. Tipton, W.J.; A.E. Fritzsche; R.J Jaffe.; Villaire A.E. *An In Situ Determination of* ^{241}*Am on the Enewetak Atoll.* Report No. EGG-1183-1778, 1981; EG&G, Las Vegas, Nevada.

17. *Environmental Radiation Measurements, Recommendations of the National Council on Radiation Protection and Measurements*. Report No. 50, 1976; pp 32 – 34. Washington D.C.

18. Beck, H.L.; J. DeCampo; C. Gogolak. *In Situ Ge(Li) and NaI(Tl) Gamma Ray Spectrometry.* Report No. HASL-258, TID-4500, 1972; U.S. AEC Health and Safety Laboratory, New York, New York.

19. Reiman, R.T. *In Situ Surveys of the U.S. Department of Energy's Rocky Flats Plant, Golden, Colorado*. Report No. EGG-10617-1129, 1991; EG&G/EM, Las Vegas, Nevada.

DISTRIBUTION

NRC/HQ

E.D.	Weinstein	(1)

NRC/REGION I

F.	Fernandez	(1)
P.D.	Kaufman	(7)
B.	Norris	(1)

DOE/DP

L.E.	Gordon-Hagerty	(1)

DOE/NV

K.D. Lachman	(1)
Public Reading Room	(1)
TIRC	(1)

NEW YORK POWER AUTHORITY (FitzPatrick)

G.	Brownell	(2)

NIAGRA MOHAWK POWER COMPANY (Nine Mile Point)

G.D.	Baker	(2)

BN

R.G.	Best	LVAO	(1)
P.P.	Guss	WAMO	(1)
R.E.	Kelley	LVAO	(1)
K.R.	Lamison	LVAO	(1)
J.T.	Mitchell	LVAO	(1)
A.E.	Proctor	LVAO	(40)
L.G.	Sasso	LVAO	(1)

LIBRARIES

RSL	(30)
WAMO	(1)

OSTI (2)